X-764-73-1
PREPRINT

NASA TM X- 66178

OPTICAL TRANSMISSION MEASUREMENTS ON MONOCRYSTALLINE AND POLYCRYSTALLINE CESIUM IODIDE

WALTER VIEHMANN
MANFRED SIMON
JOHN F. ARENS

JANUARY 1973

GSFC — GODDARD SPACE FLIGHT CENTER
GREENBELT, MARYLAND

X-764-73-1

OPTICAL TRANSMISSION MEASUREMENTS ON MONOCRYSTALLINE AND POLYCRYSTALLINE CESIUM IODIDE

Walter Viehmann and John F. Arens
Goddard Space Flight Center
Greenbelt, Md., 20771

and

Manfred Simon*
Max Planck Institut fur Extraterrestrische
Physik, Munich, Germany

January 1973

*Present Address: Goddard Space Flight Center, Greenbelt, Md. 20771, Code 661.

GODDARD SPACE FLIGHT CENTER
Greenbelt, Maryland

CONTENTS

ILLUSTRATIONS

ILLUSTRATIONS (Continued)

TABLES

Sample Nr.	Identification
I.	Single x-tal, (Tl). (Arlene's)
II.	Single x-tal (Na); Carol
III.	Single x-tal, (Na); Harshaw, Dr. Scheepmaker
IV. 1 through 5	Single x-tal, (Tl); Quarz & Silice, LSU;
V.	Polyscin; Harshaw, accidental double doping ?
VI.	Polyscin, Harshaw, accidental double doping ?
VII.	Polyscin, (Na); Harshaw, (cylinder)
VIII.	Polyscin, (Na) Harshaw; Dr. Scheepmaker
IX.	Hot-pressed pellet (IR); Fred Gross
X.	Single x-tal; Tl; Teledyne/Isotopes; Marshall

OPTICAL TRANSMISSION MEASUREMENTS ON MONOCRYSTALLINE AND POLYCRYSTALLINE CESIUM IODIDE

I. INTRODUCTION

This report is a summary of optical measurements performed on a variety of Cesium-Iodide, (CsI), samples in an effort to characterize quantitatively the optical quality of state-of-the-art material and to define and measure parameters which determine it's suitability as a detector material for the High Energy Cosmic Ray Experiment, (HECRE) on HEAO-A. This experiment has been designed to measure the intensities of protons, electrons, α-particles and heavier nuclei in the energy region from 10^{10} to 10^{14} eV. One of the sensors contains two Cesium-Iodide modules, each of which consists of five slabs of CsI of 38 cm x 38 cm x 2 cm dimensions. The square CsI slabs are each symmetrically coupled to two Photomultiplier tubes by means of air light-guides attached to two of the narrow end faces of the CsI scintillation crystal. Sensitivity and resolution depend on the efficiency with which light generated in the scintillator is transmitted to the PMTs by repeated internal reflections. This efficiency, in turn, depends on the optical quality of the CsI material. Previous experience with CsI slabs of the size contemplated here is non-existent. The results obtained in this investigation will therefore, form the basis for detector material specifications and aid in the selection and acceptance of suitable CsI material for the High-Energy Cosmic Ray Experiment. In accordance with this objective, the following measurements were performed:

1. Transmission as a function of wavelength of commerically available CsI samples which are representative of the state-of-the-art.

   a. as received

   b. after re-polishing

   c. after encapsulation into Lucite and Silicone oil

2. Laser-beam measurements of transmission on large samples of dimensions comparable to those of the HECRE modules.

   a. under normal incidence

   b. under multiple internal reflections

3. Attenuation length measurements, characterizing the volume absorption as a function of wavelength.

Measurements were made on Sodium-activated and Thallium-activated single crystals and on polycrystalline samples of the "Polyscin"* type.

The samples available for this study were numbered for identification purposes, Further information pertaining to manufacturer, history and ownership will be supplied upon request.

II. THEORETICAL ASPECTS AND DEFINITION OF PARAMETERS

The general case of light transmission through a long rectangular slab under multiple internal reflections is schematically illustrated in Figure 1. Transmission, defined as the ratio of transmitted to incident intensity, is determined by reflection and scattering losses at each interface between optical media of different indexes of refraction, and by volume-absorption and volume-scattering losses in the optical material. In first order approximation*** one obtains for the transmission:

$$T = \frac{I_{trans}}{I_{inc.}} = (1 - R_1)^2 \times (1 - S_1)^2 \times R_2^N \times (1 - S_2)^N \times e^{-k\ell} \qquad (1)$$

where R_1 and R_2 are the reflectivities at the end surfaces and side surfaces, respectively, S_1 and S_2 the corresponding scattering coefficients, N the number of internal reflections, ℓ the optical path length and k the effective absorption coefficient.** The inverse of K, $1/k = \ell_o$, is usually referred to as the absorption length.

In calculating theoretical transmission curves as a function of the number of internal reflections, we have assumed ideal conditions, namely $R_2 = 1$ (total internal reflection), $k \times \ell \ll 1$, (no internal losses) and $S_1 = S_2 = 0$, (no scattering losses at the interfaces). Then equation (1) reduces to the simple form:

$$T = (1 - R_1)^2 \qquad (1a)$$

where R_1 is a function of the indexes of refraction and of the angle of incidence commensurate with the number of internal reflections.

---

*Harshaw Trade Name.

**No formal distinction is made between scattering-losses and absorption in the bulk material.

***For $R_1(\theta) > 0.2$ a second order correction in the form of the factor $(1 + R_1^2)$ was added.

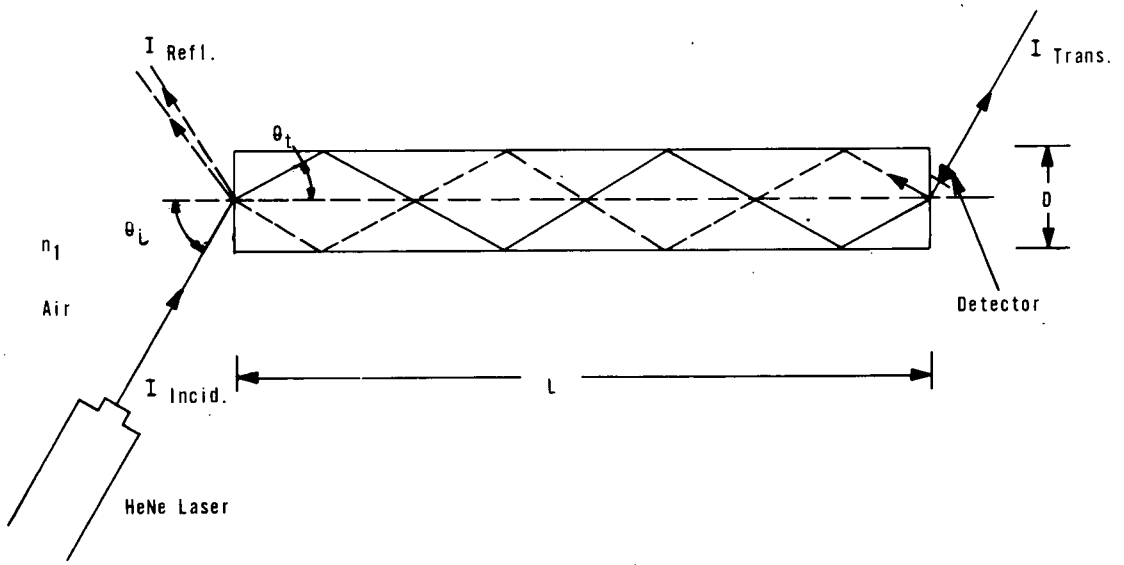

Figure 1. Schematic of Transmission and Reflection under Multiple Internal Reflection

Based on geometrical considerations, Snell's Law, and the Fresnel Equations we obtain the following set of equations for calculating R_1,

$$\text{tg}\,\theta_t = N\frac{D}{L} \tag{2}$$

$$n_1 \sin\theta_i = n_2 \sin\theta_t \tag{3}$$

$$r_{\parallel} = \left(\frac{E_r}{E_i}\right)_{\parallel} = \frac{n_2 \cos\theta_i - n_1 \cos\theta_t}{n_2 \cos\theta_i + n_1 \cos\theta_t} \tag{4a}$$

$$r_{\perp} = \left(\frac{E_r}{E_i}\right)_{\perp} = \frac{n_1 \cos\theta_i - n_2 \cos\theta_t}{n_1 \cos\theta_i + n_2 \cos\theta_t} \tag{4b}$$

$$R = \frac{1}{2}\left(r_{\parallel}^2 + r_{\perp}^2\right) \tag{5}$$

and because of symmetry,

$$R\,(n_1 \rightarrow n_2) = R\,(n_2 \rightarrow n_1) = R_1 \tag{6}$$

The symbols have the following meaning:

N = number of internal reflections

D = width of slab

L = length of slab

n_2 = index of refraction of slab

n_1 = index of refraction of surrounding medium

E_r, E_i = amplitudes of reflected and incident light for parallel ($\parallel$) and perpendicular ($\perp$) polarization, respectively

θ_i = angle of incidence and

θ_t = angle of refraction.

For CsI encapsulated into Lucite (n = 1.5) and Silicon Oil (n = 1.54), two transitions, air-Lucite — CsI (n = 1.8), were taken into account.

III. INSTRUMENTATION AND MEASUREMENT TECHNIQUES

Samples whose largest dimension did not exceed 10 cm were measured under normal incidence in a Carey 14 Spectrophotometer over the wavelength range of 250 nm to 650 nm. Transmission measurements on large samples were performed in a bench set-up, utilizing a HeNe laser of nominally 1 milliwatt output at $\lambda = 633$ nm. In the multiple internal reflection mode, (see Figure 1), measurements were made with a beam diameter of 1 mm and a square, 2.5 cm x 2.5 cm Silicon Solar cell as detector. The beam was chopped at 500 Hz and the detector output into a 10 Ω load resistor was measured with a lock-in amplifier. For normal-incidence measurements, the beam was expanded and collimated to a diameter of $\geqslant 10$ mm and a measurement beam of 8 mm diameter was defined by means of a circular aperture. In this mode, transmitted intensity was measured with a circular Si-Photodiode of 10 mm entrance aperture. In all measurements the detectors were placed as close as possible to the sample in order to avoid errors due to beam deflection and beam deformations resulting from non-parallel and non-flat end faces and internal stresses.

IV. RESULTS AND DISCUSSION

Small Samples; ($k\ell \ll 1$)

A. Transmission and scattering as a function of wavelength at normal incidence.

Spectral transmission curves recorded on a number of single crystals and on Polyscin samples are shown in Figures 2a, 2b, 2c, and 2d. The majority of our samples did not exhibit any structure in their transmission curves, i.e.,

there were no indications of absorption-peaks indicative of impurities or color centers below the absorption edge. Exceptions to this were found in Tl-activated single crystals Nr. IV, 2 and IV, 3 (see Figure 2d) and the polyscin samples Nr. V and VI.

The former exhibited four well defined absorption peaks at approximately 390 nm, 460 nm, 520 nm, and 560 nm, respectively, and the latter a single broad shoulder centered at approximately 425 nm. Under UV-excitation, the emission spectra of these polyscin-materials showed two broad peaks, one at about 420 nm, which is characteristic of Na-activated CsI, and one at about 560 nm, indicative of Tl-activated CsI. The single crystal samples Nr. IV, 2 and IV, 3, on the other hand, exhibited the typical Tl-emission spectrum. The cause of these absorption peaks was not further pursued in the course of this investigation.

In general, for optical path lengths of the order of a few centimeters, attenuation is entirely dominated by reflection — and scattering losses at the surfaces. Transmission, therefore, does not correlate with sample thickness but is strongly dependent on the quality of the surface polish. In the "as received" condition, surface polishes of the various samples available for this study ranged from "fair" to "poor", usually as the result of inadequate handling procedures or prolonged storage in ambient atmosphere. A number of samples were, therefore, lapped and polished according to the procedure described in Appendix A to a surface condition which we consider to be representative of the best possible optical finish for CsI, and measured with minimum delay after polishing. In addition, in order to simulate the encapsulation of CsI into Lucite and Silicone Oil, various samples were covered with a thin film of oil and sandwiched between a pair of 1.6 mm thick Lucite plates.

Table I summarizes the results of the measurements performed on short path-length samples in the Carey 14. In all samples, transmission decreases markedly with decreasing wavelength and more so for "poor" polish than "good" polish. For well polished surfaces, scattering coefficients, S_1, as determined, according to equation (1) from measured transmission values and calculated reflectivities, are typically of the order of 0.1 in the red and 0.2 in the blue wavelength region and up to 0.3 and 0.45 in the red and blue, respectively, for poorly polished or degraded surfaces.

Encapsulation reduces scattering and improves transmission dramatically over the whole wavelength range, (see Figure 2). The relative improvement is higher in the blue than in the red and higher for poorly polished surfaces than for well polished samples. (The UV cut-off at $\sim$350 nm is due to the UVA grade Lucite.

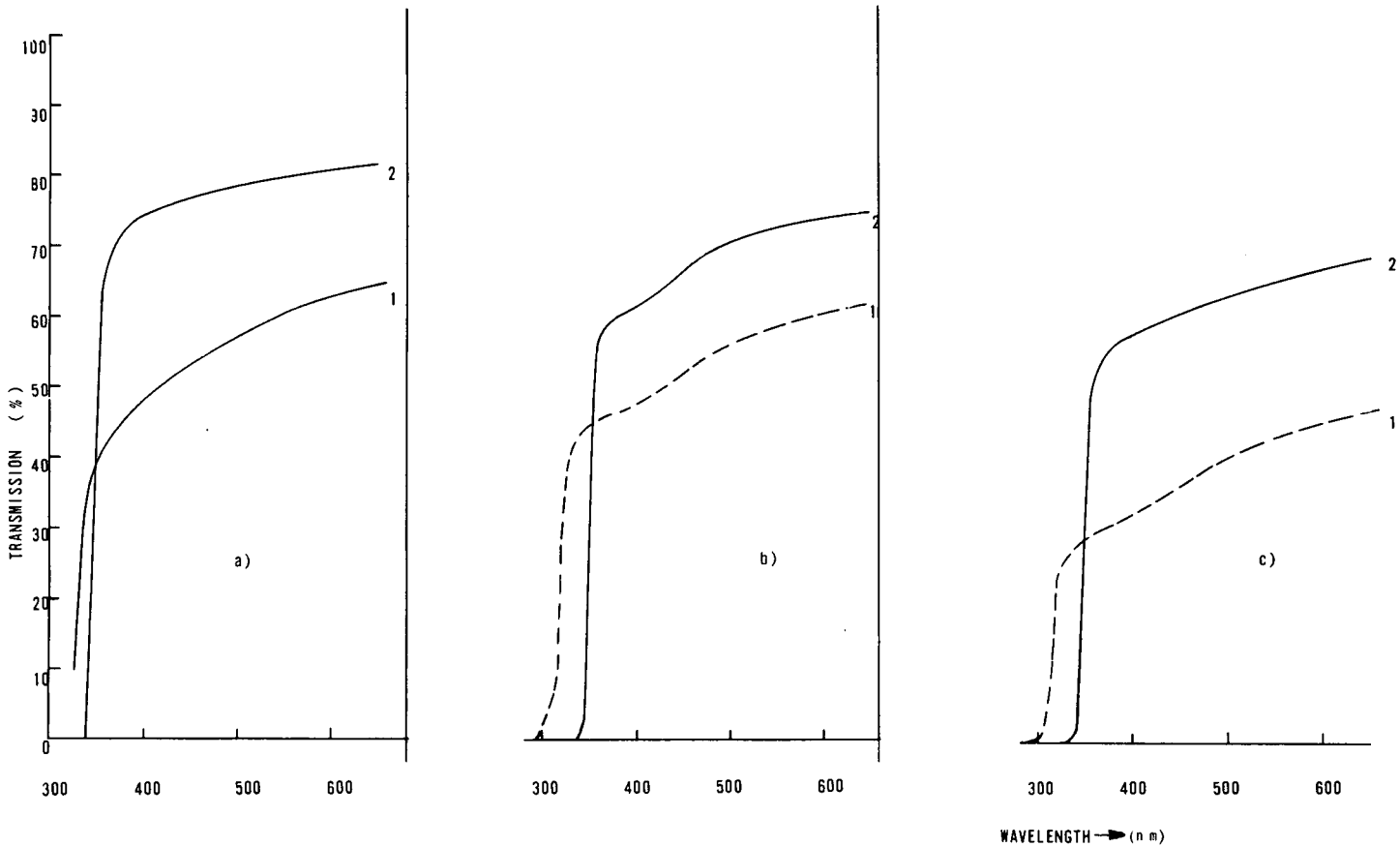

Figure 2. Transmission of CsI Samples as a Function of Wavelength

a. Tl-activated single crystal, encapsulated in Si-Oil and Lucite (upper curve) and not encapsulated (lower curve); optical path length = 2.7 cm.

b. Polyscin; encapsulated (upper curve); not encapsulated (lower curve) optical path-length = 5 cm.

c. Polyscin; same sample as in 2b; encapsulated (upper curve); not encapsulated (lower curve); optical path-length = 2 cm.

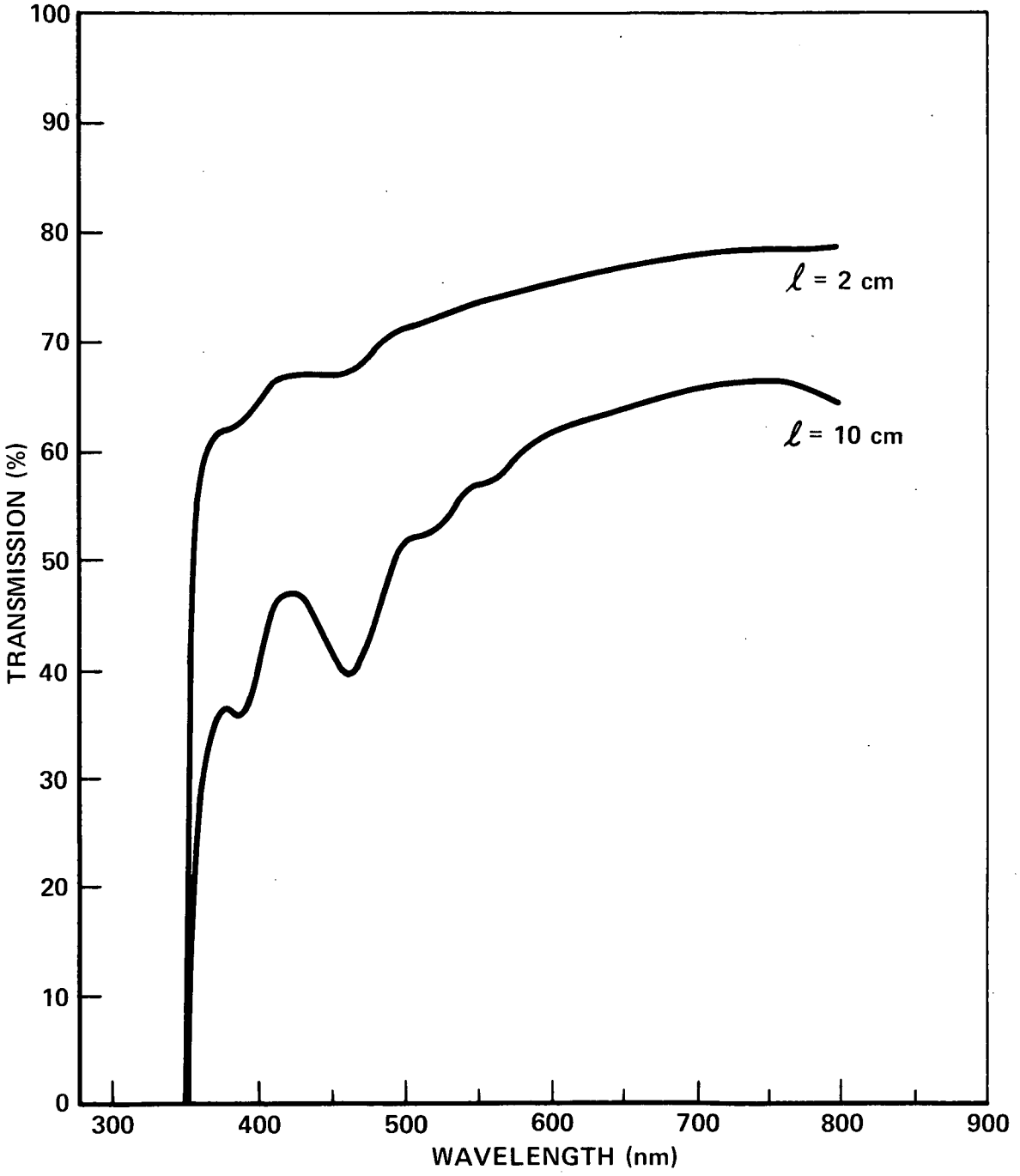

Figure 2. Transmission of CsI Sample as a Function of Wavelength

d. Encapsulated Tl-Activated Single Crystal, Sample #IV, 2; Optical Path-Length = 2 cm (Upper Curve) and 10 cm (Lower Curve).

Table I
Transmission and Scattering of Short Path-Length Samples Under Normal Incidence

Sample No.	Remarks		Transmission %		$\frac{T_{red}}{T_{blue}}$	Surface Scattering % Normal Incidence		$\frac{T_{encaps}}{T_{unencaps}}$		$\frac{S_{1\ blue}}{S_{1\ red}}$
	Surface Quality	Optical Path (cm)	$T_{625\,nm}$	$T_{425\,nm}$		S_1 (625nm)	S_1 (425nm)	625nm	425nm	
I CsI (Tl) Single Crystal 2.5cm dia x 2.7cm	Poor Repolished Polished and Encapsulated	2.70	58 63 81	39 51 75	1.50 1.23 1.08	17 14 6	32 23 9	— — 1.30	— — 1.47	1.88 1.64 1.50
II CsI (Na) Single Crystal 2.5cm dia x 2cm	Good	2.00	69	53	1.30	10	21	—	—	2.10
III CsI (Na) Single Crystal 1.9cm x 4.13cm x 20cm	Encapsulated	4.13	75	72	1.04	9	11	—	—	1.22
IV CsI (Tl) Single Crystal 10cm x 10cm x 2cm	Encapsulated	2.00				(a)	(a)			(a)
IV. 1			76	73	1.04	9 (8)	11 (10)	—	—	1.22 (1.25)
IV. 2			76	68	1.12	9 (7)	14 (10)	—	—	1.55 (1.42)
IV. 3			70	64	1.10	12 (10)	16 (11)	—	—	1.33 (1.10)
IV. 4			83	75	1.10	5 (4)	8 (6)	—	—	1.60 (1.50)
IV. 5			76	73	1.04	9 (4)	10 (4)	—	—	1.11 (1.00)
V Polyscin (Na, Tl) 2cm x 4cm x 5cm (b)	Good	5.00	62	50	1.24	15	23	—	—	1.53
	Poor	4.00	43	32	1.35	29	39	—	—	1.34
	Poor	2.00	46	35	1.31	26	36	—	—	1.38
	Encapsulated	5.00	75	64	1.17	10	16	1.20	1.28	1.60
		2.00	68	60	1.14	14	19	1.47	1.70	1.36
VI Polyscin (Na, Tl) 2cm x 4cm x 5 cm (b)	Fair	5.00	51	39	1.30	23	33	—	—	1.43
	Poor	4.00	37	28	1.32	34	44	—	—	1.29
	Fair	2.00	53	42	1.25	21	30	—	—	1.43
VII Polyscin (Na) 4.5cm dia x 6.4cm	Fair	6.40	49	41	1.20	24	30	—	—	1.25
	Encapsulated	6.40	76	70	1.08	9	12	1.55	1.70	1.33
VIII Polyscin (Na) 38cm x 1.9cm x 4.13cm	Fair to Good	4.13	51	43	1.20	23	29	—	—	1.29
	Encapsulated		65	58	1.12	15	20	1.27	1.35	1.33
IX CsI Hot-Pressed Pellet 1.2cm dia x 0.2cm	Unencapsulated	0.20	61	52	1.17	15	22	1.30	1.45	1.46
	Encapsulated		80	75	1.07	7	9			1.38
X Lucite	—	0.60	91	91	1.00	0.5	0.5			

(a) Values in paranthesis are corrected for volume absorption
(b) Nominal activation was Na, but emission spectrum indicated Tl activation as well.

UVT-grade, or UV transmitting Lucite, transmits to about 300 nm.) For well polished, encapsulated material, scattering coefficients are as low as 0.06 in the red and 0.09 in the blue. These values should be compared to scattering coefficients of $\leqslant 0.01$ for optical grade Lucide and $\leqslant 0.001$ for optical glasses. It should also be noted, that the lowest scattering coefficients measured on encapsulated Polyscin are only slightly higher than those for encapsulated single crystals. However, it is important to point out, that low scattering coefficients were only observed on the small surfaces of the bar-shaped Polyscin samples and that those for the large surfaces were higher by a factor of approximately 1.5. We can only surmise that this relates to the (proprietary) preparation process, and we want to stress that we were unable to improve Polyscin surfaces by the wet polishing process successfully applied to single crystals as described in Appendix A.

As a measure of the wavelength dependence of scattering, the ratios of S_1 at 425 nm to S_1 at 625 nm are listed in Table I for all samples measured in the Carey 14. They range from a low of 1.0, (S independent of λ), to a high of 2.1, ($S \sim \lambda^{-2}$) with a mean value of ~ 1.35, i.e., on the average, S is very nearly proportional to λ^{-1}.

B. Angular Distribution of Scattered Intensity

Figure 3 shows the angular distribution of scattered intensity for a typical CsI sample and for a glass sample of intentionally poor surface polish. We note that back-scattering is negligible compared to forward scattering and that the latter is concentrated in a small cone around the incident beam with a cone angle of about 12 to 15 degrees, or a solid angle of 35 to 45 milli ster radians. In the laser-beam measurements, forward scattering from the surface closest to the detector is measured as transmission, whereas the spectrophotometer results represent "true" transmission values by virtue of excluding practically all scattered light. Attempts to perform "correct" transmission measurements in the laser set-up by placing appropriate apertures in front of the detector were discarded, as it was noted that — particularly on long path-length samples — serious errors could occur due to de-collimation and refraction of the beam if the end faces were not optically flat and parallel. For laser measurements, scattering coefficients were therefore determined according to $I_{tr}/I_{inc} = (1-S)(1-R_1)^2$, as compared to $(1-S)^2\ (1-R_1)^2$ for Spectrophotometer measurements, resulting in good agreement between the two methods.

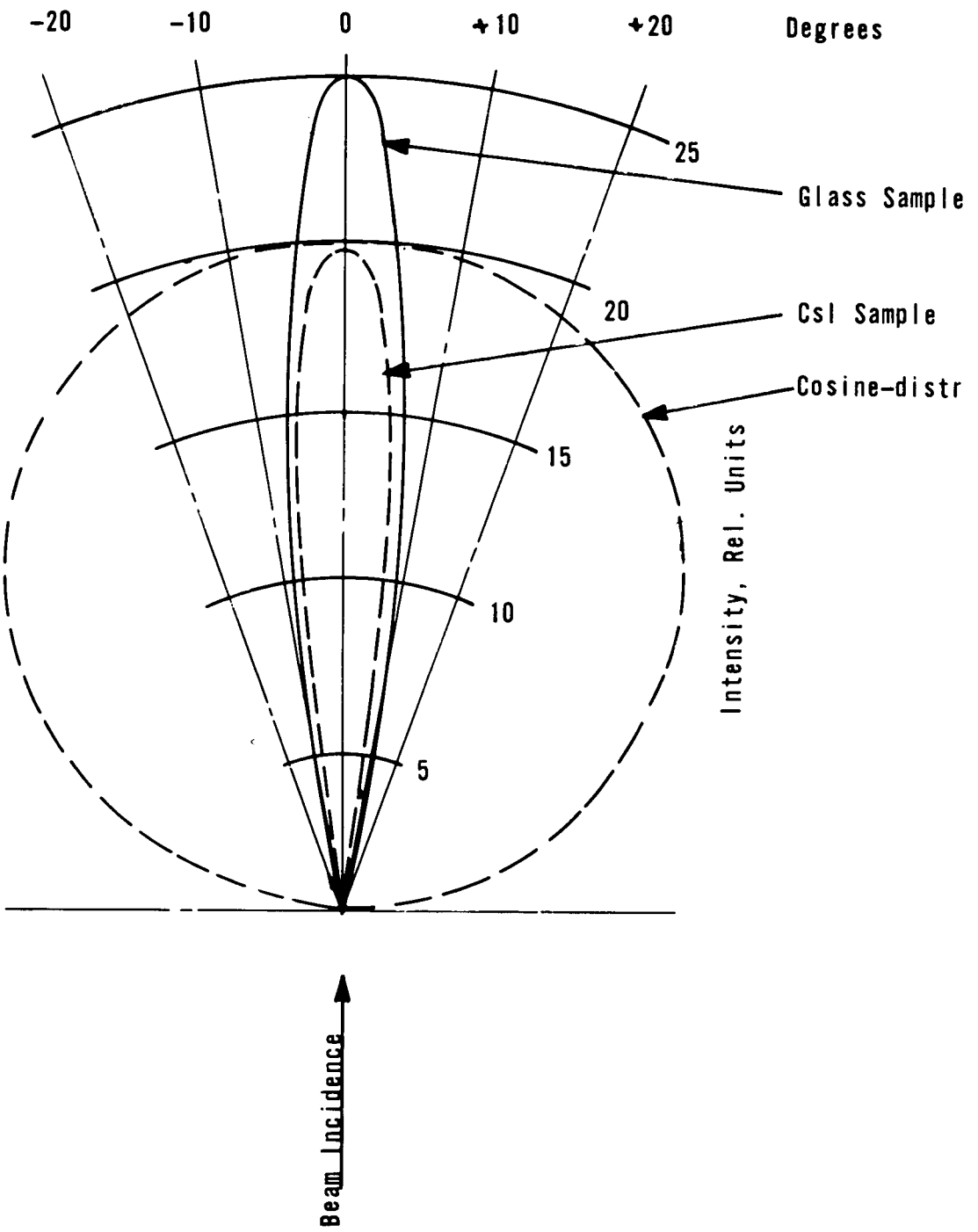

Figure 3. Angular Distribution of Scattering; with Cosine-Distribution for Comparison; Backscattering $\leq 1\%$ of Forward Scattering. Detector Solid Angle, $\Omega = 7 \times 10^{-4}$ Ster.

Large Samples

Five encapsulated single crystals* of Tl-activated CsI, each of 10 cm x 10 cm x 2 cm dimensions, one large crystal, Tl-activiated and of 23 cm x 23 cm x 1.25 cm dimensions, and three bar-shaped pieces of Polyscin, one 38 cm x 4.13 cm x 1.9 cm and two each of 5 cm x 4 cm x 2 cm dimensions, were available for the determination of volume-absorption coefficients and transmission measurements under total internal reflections in addition to those measurements already described for small samples. In particular, where size permitted, normal incidence measurements were made in both the spectrophotometer as a function of wavelength, as well as in the laser set-up at $\lambda = 633$ nm.

A. Normal Incidence; Surface Scattering and Volume Absorption

By measuring transmission under normal incidence through two widely different path-lengths, ℓ_1 and ℓ_2, and assuming reflection and scattering losses on all four surfaces to be identical, one obtains the absorption coefficient according to equation (1) as:

$$k = \frac{1}{\ell_2 - \ell_1} \ln \frac{I_{tr}(\ell_1)}{I_{tr}(\ell_2)} \tag{7}$$

Table II summarizes the results thus obtained from both the spectrophotometer and the laser measurements. For the latter, a minimum of 20 measurements were made at different locations for each path length in order to obtain a measure of the uniformity in volume absorption for the various samples. Accordingly, Table II lists the average value for k, a minimum and maximum value, corresponding to the lower and upper 10% of the distribution, respectively, and the measurement uncertainty associated with the average. The spectrophotometer measurements, on the other hand, represent single point values near the center of the samples, and should be viewed with the statistical variation in mind, established by the laser measurements.

The main purpose of the single point measurements was to establish the wavelength-dependence of the absorption and scattering coefficients. Of particular interest are the values of k at $\lambda = 425$ nm, the wavelength of the fluorescense emission peak of Na-activiated CsI. For all samples, the absorption coefficient increases with decreasing wavelength. Although some of the ratios of k (425 nm)/k(625 nm) listed in Table II could be fortuitous, because the spectrophotometer

*The term "single crystal" is used rather loosely here, as most samples consisted of a few large crystallites separated by readily discernible grain boundaries.

Table II

Absorption Coefficient, k, and Absorption Length, 1/k, of Large CsI Samples

Sample Nr	λ = 633 nm. k (10^{-2} cm^{-1})					1/k (cm) (average)	λ = 425 nm. k (10^{-2} cm^{-1})	$\frac{k_{blue}}{k_{red}}$ (Carey)
	$k_{average}$ Laser	$k_{average}$ Carey	k_{min}	k_{max}	Uncertainty %		Carey	
Single Crystals, CsI (Tl), 10 cm x 10 cm x 2 cm								
IV. 1	0.75	0.8				133	0.95	1.18
IV. 2	2.80	2.3	2.3	3.60	± 6	36	4.30	1.87
IV. 3	2.40	2.8	1.8	3.00	± 9	42	5.80	2.07
IV. 4	0.60	2.0	0.5	0.65	± 11	167	2.90	1.45
IV. 5	4.30	5.0	3.6	5.20	± 5	23	7.40	1.48
X. CsI (Tl) single Crystal 23 cm x 23 cm x 1.25 cm	1.00	—	0.3	3.30	± 8	100	—	—
V. & VI. Polyscin	2.80	5.5	2.0	3.70		36	8.00	1.45
VIII. Polyscin	<0.20	—	—	—		>500		

results are not statistical averages, it seems safe to conclude that this ratio is on the average about 1.5, so that similarly to the surface scattering coefficients, the volume "absorption" is also proportional to λ^{-1}.

It is apparent from Table II, that the five 10 cm x 10 cm x 2 cm pieces (samples Nr. IV, 1 to IV, 5) are quite uniform in themselves, but that considerable variations exist from piece to piece, with k at λ = 633 nm ranging from a low of 1 x 10^{-2} cm^{-1}, corresponding to an attenuation length of 100 cm, to a high of 5 x 10^{-2} cm^{-1}, or 20 cm attenuation length. Within sample Nr. X (23 cm x 23 cm x 1.25 cm), k varies by an order of magnitude, from 0.3 x 10^{-2} cm^{-1}, for good sections (ℓ_0 = 335 cm), to a high value of 3.3 x 10^{-2} cm^{-1}, corresponding to attenuation length of 30 cm, for poor sections. Similarly, for the small bars of Polyscin, (samples Nr. V and VI), k was found to be ~ 3 x 10^{-2} cm^{-1}, whereas for the large bar of Polyscin (sample Nr. VIII) it was as low as, or lower than, 0.2 x 10^{-2} cm^{-1}, which is smaller than the best value measured on single crystals. It is worth noting, then, that the volume "absorption" of both single crystal material and of Polyscin varies by approximately an order of magnitude from sample to sample, as well as within large pieces, presumably as the result of varying growth or preparation conditions. It should be emphasized, therefore, that a careful screening process would seem to be mandatory for selecting high-quality samples.

B. Transmission Under Total Internal Reflection

1. Single Crystals

Figure 4 shows the transmission of the 23 cm x 23 cm x 1.25 cm slab of CsI as a function of the number of internal reflections as measured in the as-received condition, after re-polishing and after encapsulation into Lucite and Silicone Oil. Measurements on a 25 cm x 25 cm x 1.25 cm Lucite plate are shown for comparison, as well as theoretical curves computed according to equations (2) to (6). Since volume absorption is small, surface scattering is the dominant factor determining transmission properties. This is readily apparent from the drastic improvements in transmission resulting from re-polishing and in particular from encapsulation. By analyzing the measured transmission curves in terms of parameters defined in equation (1), one obtains for $N \leq 4$ scattering coefficients, S_2, of approximately 0% for the as-received condition, 11% after re-polishing and 8% after encapsulation of the re-polished material. For Lucite, S_2 is ~ 1.5%.

We note that the scattering coefficients, S_2, for re-polished and encapsulated material are about a factor of 1.5 higher than the lowest scattering coefficients, S_1, obtained under normal incidence on well polished, encapsulated single crystal samples, (see Table I).

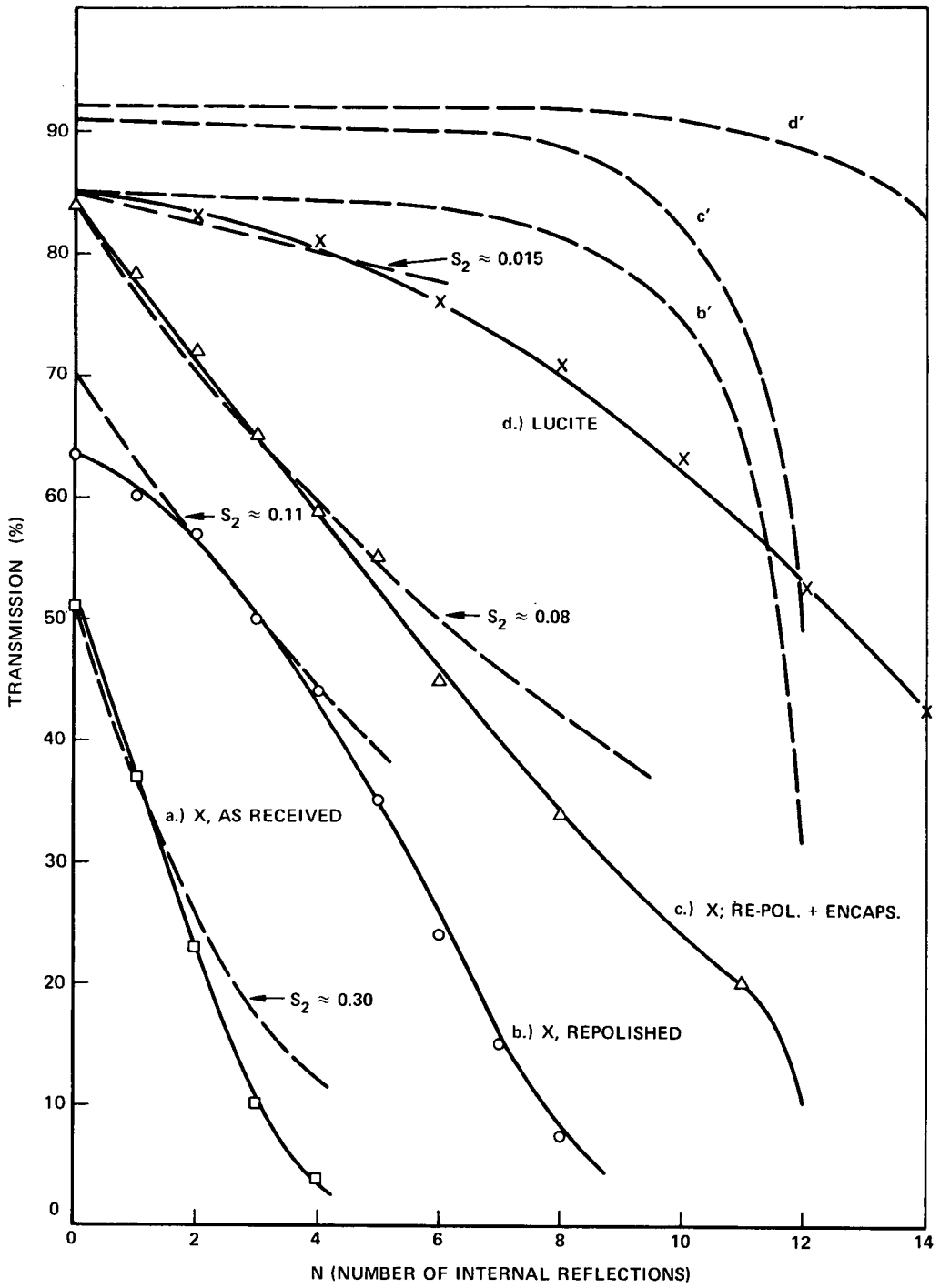

Figure 4. Transmission as a Function of the Number of Internal Reflections for CsI Sample Nr. X. (L = 23 cm, D = 1.25 cm, λ = 633 nm, Beam Diameter = 1 mm). Theoretical Curves (Broken Lines) are Shown for Comparison.

For $N \geq 4$ transmission decreases somewhat faster with increasing number of internal reflections than one would compute according to equation (1) with constant scattering coefficients. On the 10 cm x 10 cm x 2 cm samples, the discrepancy between S_1-values determined under normal incidence and S_2-values obtained from measurements under internal reflections is particularly pronounced, as can be seen from Figure 5. Values for S_2 are approximately twice as high as S_1 values for these samples. It should be noted at this point that because of the smaller length to thickness ratio of samples Nr. IV, the angles of incidence and reflection for N = 1 to N = 3 are those that occur in the larger samples Nr. X at N = 6 to N = 8. At these angles of internal reflection the increase of S_2 becomes pronounced, with S_2 being about twice as high as S_1.

2. Polyscin

Internal reflections on the Polyscin sample occurred on the large faces of the rectangular bar. As was pointed out previously, these surfaces were found to have significantly higher scattering coefficients than the small surfaces. For encapsulated samples, S_1-values determined in the spectrophotometer under normal incidence are in the range of 15% to 20% for these surfaces, as compared to 9% to 14% for the small surfaces. Transmission under internal reflection is shown in Figure 6 for "good" areas and "bad" areas of Polyscin, with theoretical curves and measurements on the best single crystal sample included for comparison. We note again, that scattering coefficients under internal reflection are higher than for normal incidence and that they increase with increasing number of internal reflections, i.e., with decreasing angle of reflection. In addition, it is quite apparent, that surface quality of Polyscin is substantially inferior to that of well polished single crystals.

V. CONCLUSIONS

In the geometrical configuration as presently conceived for the CsI-modules of the HEAO-A High Energy Cosmic Ray Experiment, light created in the scintillator crystal will on the average undergo five internal reflections and travel a distance of approximately 20 cm through the crystal before entering the light-guide/PMT structures at opposite end faces of the CsI slab. As a "figure of merit", we therefore define the quantity

$$F = (1 - R_1)(1 - S_2)^5 \, e^{-k\ell},$$

describing the relative collection efficiency of a scintillator crystal in the total internal reflection mode. R_1, S_2 and k are the previously defined reflection, — scattering—, and absorption coefficients, respectively.

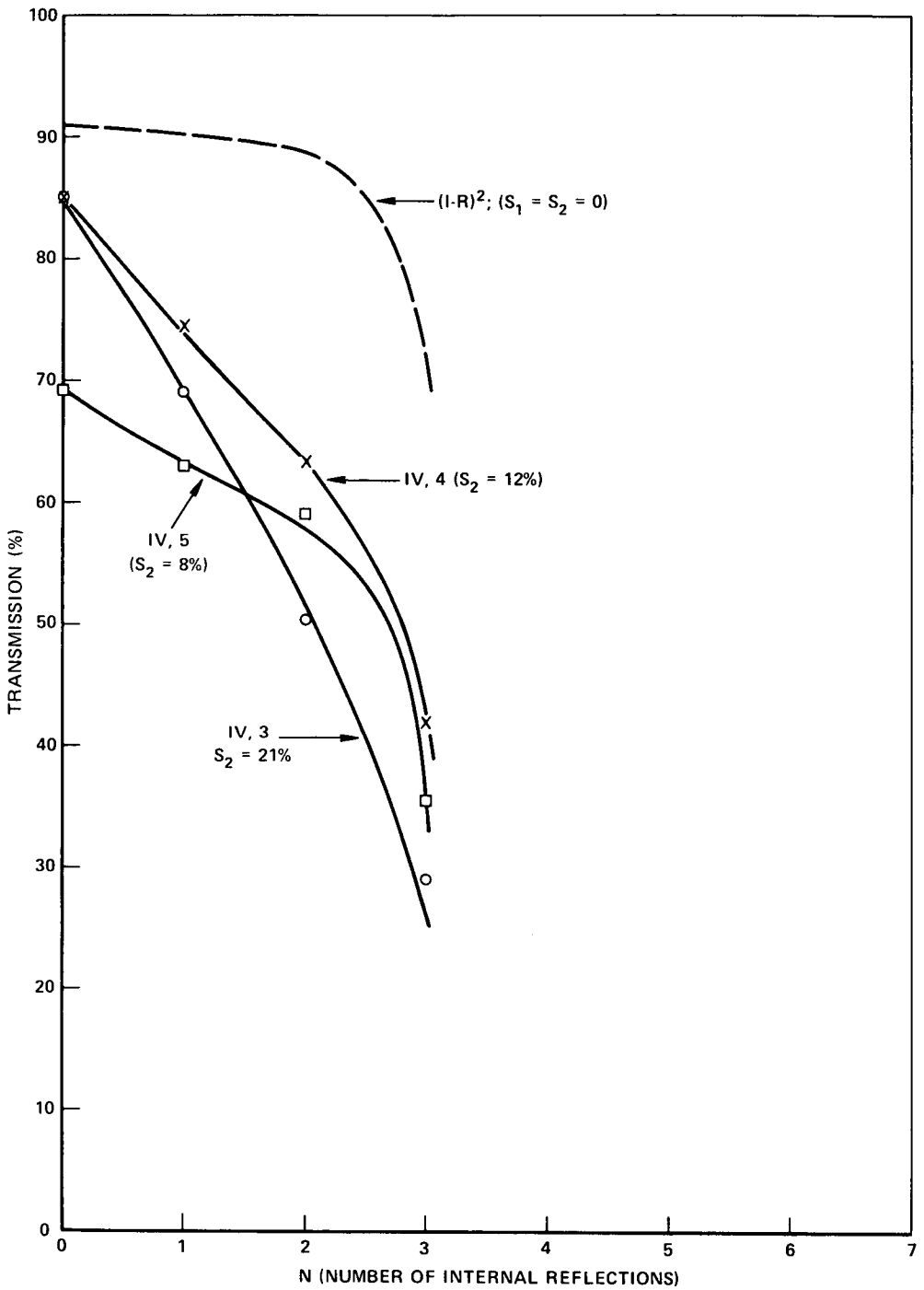

Figure 5. Transmission Under Total Internal Reflection as a Function of the Number of Reflections for 3 Samples of Encapsulated CsI: (L = 10 cm; D = 2 cm; λ = 633 nm; Beam Diameter = 1 mm) Ideal Theoretical Curve (Broken Line) Shown for Comparison.

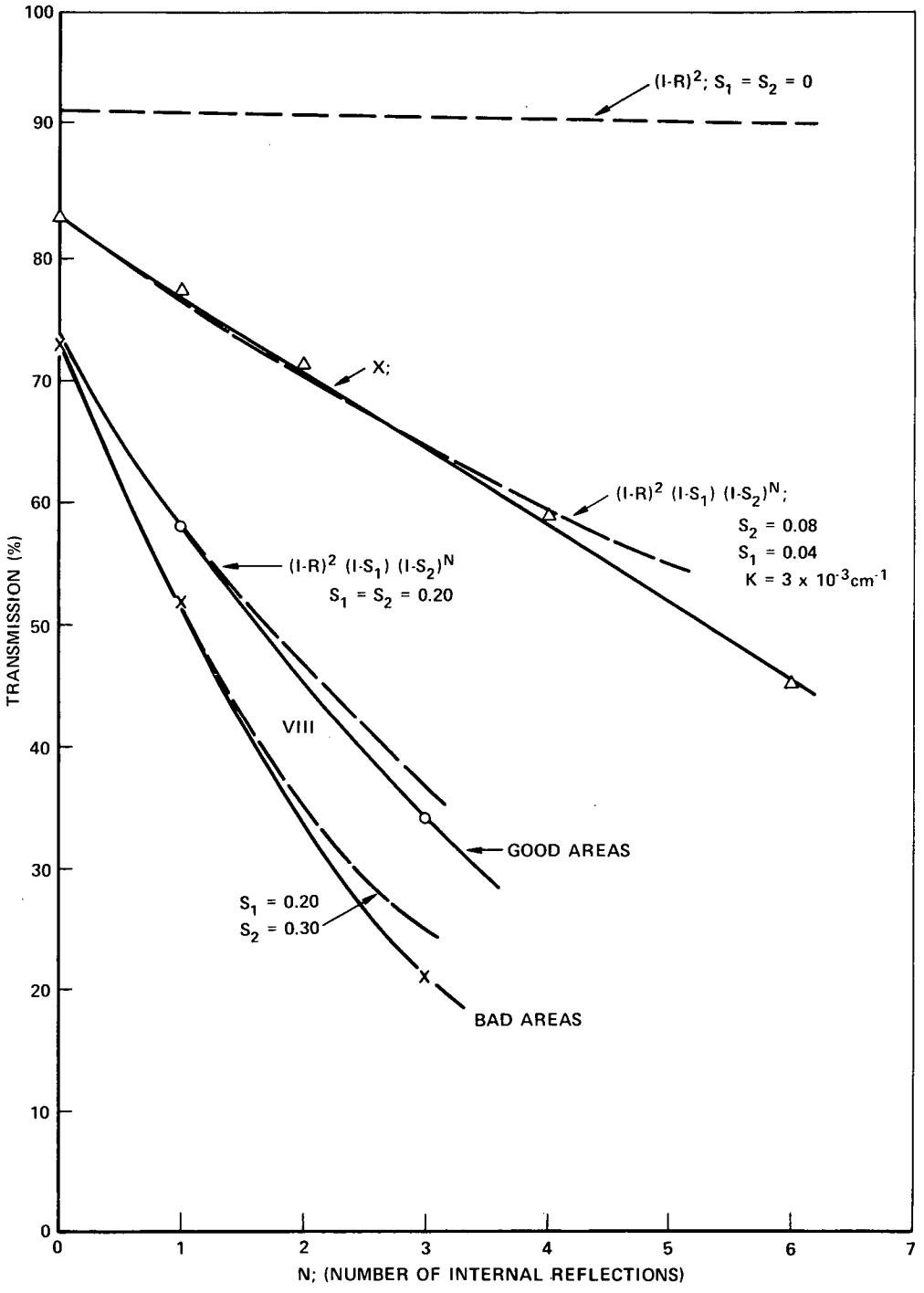

Figure 6. Transmission Under Internal Reflection for Polyscin Sample. (L = 38 cm; D = 1.9 cm; λ = 633 nm; Beam Diameter = 1 mm). Ideal Theoretical Curve (Broken Line) and Measurements on Single Crystal Sample #X, are Shown for Comparison.

Tables III and IV list numerical values for these coefficients for the red and blue wavelength region, that—based on our measurements—can be considered as typical for good, average, and poor quality single crystal and polycrystalline material, respectively, and the figures of merit resulting from these values. (Scattering losses at the end faces have not been included in F, since scattering is entirely in the forward direction.)

The requirement of uniformity of light collection of 2% per cm yields a lower limit for F of 0.4. In the red wavelength region, single crystal material of average quality and Polyscin of good quality meet this requirement, whereas in the blue, only good quality single crystals can be considered among present state-of-the-art materials meeting the requirement. The application of Polyscin in large CsI modules relying on total internal reflection will depend on substantial improvement of it's surface quality.

ACKNOWLEDGEMENTS

The authors would like to thank Dr. W. Schmidt of the Institut fuer Extraterrestrische Physik, Munich, for valuable discussions and suggestions. They are indebted to Ms. Jane E. Jellison for developing the polishing procedure described in the Appendix and for applying it to many of the samples used in this work. The contributions of John L. Tarpley to the handling and encapsulation techniques of large samples are also greatly appreciated.

Table III

Scattering Parameters and Figures of Merit for Red Light

$\lambda = 625\,nm$; $(1-R_1) = 0.96$				
Encapsulated Single Crystal CsI				
	$(1-S_1)$	$(1-S_2)^5$	$e^{-k\ell}$ $\ell = 20\,cm$	$F = (1-R)(1-S_2)^5 e^{-k\ell}$ $\ell = 20\,cm$
good	0.965 ($S_1 = 3.5\%$)	0.70 ($S_2 = 7\%$)	0.94 $k = 0.3 \times 10^{-2}\,cm^{-1}$	0.63
average	0.95 ($S_1 = 5\%$)	0.60 ($S_2 = 10\%$)	0.67 ($k = 2 \times 10^{-2}\,cm^{-1}$)	0.39
poor	0.92 ($S_1 = 8\%$)	0.42 ($S_2 = 16\%$)	0.37 ($k = 5 \times 10^{-2}\,cm^{-1}$)	0.14
Encapsulated Polyscin				
good	0.92 ($S_1 = 8\%$)	0.44 ($S_2 = 15\%$)	0.96 ($k = 0.2 \times 10^{-2}\,cm^{-1}$)	0.40
average	0.85 ($S_1 = 15\%$)	0.24 ($S_2 = 25\%$)	0.82 ($k = 1 \times 10^{-2}\,cm^{-1}$)	0.19
poor	0.80 ($S_1 = 20\%$)	0.12 ($S_2 = 35\%$)	0.37 ($k = 5 \times 10^{-2}\,cm^{-1}$)	0.04

Table IV

Scattering Parameters and Figures of Merit for Blue Light

$\lambda = 425\,nm$; $(1-R_1) = 0.96$				
Encapsulated Single Crystal CSI				
	$(1-S_1)$	$(1-S_2)^5$	$e^{-k\ell}$ $\ell = 20\,cm$	$F = (1-R)(1-S_2)^5 e^{-k\ell}$ $\ell = 20\,cm$
good	0.95 ($S_1 = 5\%$)	0.60 ($S_2 = 10\%$)	0.92 ($k = 0.4 \times 10^{-2} cm^{-1}$)	0.53
average	0.92 ($S_1 = 8\%$)	0.42 ($S_2 = 16\%$)	0.57 ($k = 3 \times 10^{-2} cm^{-1}$)	0.23
poor	0.88 ($S_1 = 12\%$)	0.25 ($S_2 = 24\%$)	0.26 ($k = 6.6 \times 10^{-2} cm^{-1}$)	0.07
Encapsulated Polyscin				
good	0.85 ($S_1 = 15\%$)	0.24 ($S_2 = 25\%$)	0.94 ($k = 0.3 \times 10^{-2} cm^{-1}$)	0.22
average	0.78 ($S_1 = 22\%$)	0.12 ($S_2 = 35\%$)	0.74 ($k = 1.5 \times 10^{-2} cm^{-1}$)	0.09
poor	0.70 ($S_1 = 30\%$)	0.03 ($S_2 = 50\%$)	0.22 ($k = 7.5 \times 10^{-2} cm^{-1}$)	< 0.01

APPENDIX
POLISHING CESIUM IODIDE

Jane Jellison

GRINDING

Coarse scratches are eliminated by using an appropriate grit size of emery paper moistened with ethylene glycol ($C_2H_6O_2$). Buehler 30-5024 4/0 grade (15 microns grit size) will remove all but very deep scratches. The ethylene glycol slightly attacks CsI and should not be allowed to stand on it for very long. With this particular paper, the adhesive bonding the abrasive to the paper will dissolve in the ethylene glycol creating a brown slurry. A soft facial tissue moistened with ethylene glycol may be used to rub this slurry over the crystal.

When the coarse scratches have been removed, clean the crystal by wiping with a succession of clean tissues moistened with ethylene glycol. Then clean the ethylene glycol off with methyl alcohol also applied with tissue.

INTERMEDIATE POLISHING

Moisten a pad of facial tissue with ethylene glycol and sprinkle about one half gram or so of 0.3 micron Al_2O_3. Polish with this, occasionally adding a little ethylene to the pad. Clean as before, with ethylene glycol followed by methyl alcohol. The finish will be hazy with very light scratches.

FINAL POLISHING

Moisten a pad of tissue with methyl alcohol and sprinkle a small amount ($\sim$0.1 g) zinc oxide powder on it. Rub with fairly heavy pressure over a small area of the crystal at a time, allowing the surface to dry every few seconds. Gradually the haze will disappear. Use light pressure towards the end. It may be necessary to re-wet the pad with a few drops of methanol. This final polishing procedure may have to be repeated one or more times before a haze-free finish is attained. No cleaning is necessary after this step.

NOTES

At no point apply the solvent, directly to the crystal. A spot will be etched where each drop lands. Dry grinding should be avoided. If the emery paper

starts to drag, add a little more ethylene glycol. Fingerprints will etch the crystal rather deeply. Rubber surgical type gloves are recommended. Change gloves, or wash them well with methyl alcohol, between the aluminum oxide and zinc oxide polishing steps. Avoid breathing on the polished surface when examining it closely. Store polished crystals in a vacuum or in an inert gas mixture.

☆ U.S. GOVERNMENT PRINTING OFFICE: 1972—735-966/498